



Preliminary issues associated with the next generation nuclear plant intermediate heat exchanger design

K. Natesan*, A. Moisseytsev, S. Majumdar

Argonne National Laboratory, 9700 S. Cass Ave, Argonne, IL 60439, USA

A B S T R A C T

The Next Generation Nuclear Plant, with emphasis on production of both electricity and hydrogen, involves helium as the coolant and a closed-cycle gas turbine for power generation with a core outlet/gas turbine inlet temperature of 850–950 °C. In this concept, an intermediate heat exchanger is used to transfer the heat from primary helium from the core to the secondary fluid, which can be helium, a nitrogen/helium mixture, or a molten salt. This paper assesses the issues pertaining to shell-and-tube and compact heat exchangers. A detailed thermal-hydraulic analysis was performed to calculate heat transfer, temperature distribution, and pressure drop inside both printed circuit and shell-and-tube heat exchangers. The analysis included evaluation of the role of key process parameters, geometrical factors in heat exchanger designs, and material properties of structural alloys. Calculations were performed for helium-to-helium, helium-to-helium/nitrogen, and helium-to-salt heat exchangers.

© 2009 Elsevier B.V. All rights reserved.

1. Introduction

The Next Generation Nuclear Plant (NGNP), which is an advanced high-temperature gas reactor concept with emphasis on production of both electricity and hydrogen, involves helium as the coolant and a closed-cycle gas turbine for power generation with a core outlet/gas turbine inlet temperature of 850–950 °C. In the indirect cycle system, an intermediate heat exchanger (IHX) is used to transfer the heat from primary helium from the core to the secondary fluid, which can be helium, a nitrogen/helium mixture, or a molten salt. The system concept for the very high-temperature reactor (VHTR) can be a system based on the prismatic block of the gas turbine-modular helium reactor developed by a consortium led by General Atomics in the U.S. or based on the Pebble Bed Modular Reactor (PBMR) design developed by ESKOM of South Africa and British Nuclear Fuels of U.K.

Several different potential plant design configurations for the NGNP with either direct or indirect power conversion cycles and integrated IHX designs were proposed and evaluated by Davis et al. [1]. These configurations included IHX designs in parallel or in series with the NGNP power conversion system. In the serial designs, the total primary system flow from the reactor outlet passes through the IHX where approximately 50 MWt is transferred to the intermediate loop to drive the hydrogen production process. In these designs, heat is extracted from the primary fluid at the highest possible temperature (the reactor outlet temperature) for delivery to the hydrogen production process, while the

power conversion system receives a slightly lower temperature fluid. In the parallel designs, the flow from the reactor outlet is split, with a small fraction of the flow (approximately 10%) going to the IHX to drive the hydrogen production process, while the majority of the flow is delivered to the power conversion system for electrical power production. In these designs, both the hydrogen production process and the power conversion system receive the highest possible temperature fluid. Harvego [2] has discussed the possible configurations for the design of IHX for NGNP and established the pros and cons of each configuration. Based on the design, he also established the flow rates, temperature distribution through the loops, and other IHX requirements. Based on results from his study, we have selected 900 °C reactor outlet temperature as the base case.

2. IHX design concepts

Three potential IHX design concepts, namely shell-and-tube, and two compact heat exchanger concepts, such as plate and fin and printed circuit heat exchanger (PCHE), are possible for the transfer of heat from the primary helium to the secondary system. Compared to shell-and-tube heat exchangers, the compact HXs are characterized by a large heat transfer area per unit volume of the exchanger, resulting in reduced space, weight, support structure, and material cost.

The shell-and-tube exchanger is generally built of round tubes in a cylindrical shell with the tube axis parallel to that of the shell. One fluid flows inside the tubes and the other flows across and along the tubes. The major components of this exchanger are tubes, shell, front-end head, rear-end head, baffles, and tubesheets.

* Corresponding author. Tel.: +1 630 252 5103; fax: +1 630 252 8681
E-mail address: natesan@anl.gov (K. Natesan).

One or both surfaces of the tubes could be augmented by means of surface fins to enhance the heat transfer as shown in Fig. 1.

The plate-type heat exchangers are usually built of thin plates. The plates are either smooth or have some form of corrugation which could be either flat or wavy in an exchanger. McDonald et al. [3] made a detailed review of the plate and fin heat exchanger requirements for process heat-modular helium reactor application. The review identifies several technical issues and the development of the IHX to be a formidable task.

Printed circuit heat exchangers, which can substantially reduce the size of the unit for a given thermal capacity, have the potential for application in a NGNP system. It is noted that PCHE is a commercial product developed by Heatric, a subsidiary of Meggitt (UK), Ltd. [4]. PCHE has been developed for other applications; applicability of the technology for NGNP has not been analyzed or confirmed by the manufacturer. Therefore, any analysis and results presented in this paper regarding PCHE could only be considered as preliminary. Neither thermal-hydraulic nor structural design of the PCHE for this high-temperature application has been carried out; instead the calculations presented below are obtained based on engineering-judgment assumptions made by the researchers rather than the PCHE developers. Similarly, the material considered in this study may not be compatible with a PCHE diffusion bonding fabrication process.

3. Model description

The thermal-hydraulic model has been developed to calculate heat transfer, temperature distribution, and pressure drop inside a heat exchanger (HX). The model is one-dimensional, meaning that it is assumed that all channels on one side are identical and the calculations are done for one hot channel and one cold channel. Thus, any edge effects, such as heat losses through the HX outside surfaces, are ignored. The model also assumes that the flow inside the HX is counter-flow, i.e., any heat transfer in flow distribution regions is ignored. Also the model is for single-phase fluids only and it is assumed that there is no phase transition inside the HX. Fig. 2 shows a simplified printed circuit heat exchanger configuration assumed for the model.

The model takes into account the fluid properties variation along the channel length. The channel length is divided into a number of regions. Inside each region the fluid properties are assumed to be constant, but the properties vary from region to region. For each region the heat transfer equations are solved to calculate the temperature changes in the region for both fluids. Also, the pressure drop for each region is calculated. The heat transfer equations, as well as their solutions are described elsewhere [5].

A shell-and-tube heat exchanger consists of a number of tubes placed inside a volume (shell). Although there are several types of shell-and-tube heat exchangers, only a counter-flow straight-tube design is considered in this paper. The model has the capability of taking into account the heat transfer surface enhancement by utilization of tube surface fins (Fig. 1). The effect of the fins on the heat transfer and how it is taken into account in the model is described elsewhere [5].



Fig. 1. Possible tube configurations: (a) bare tube, (b) fins on outer surface, (c) fins on inner surface, and (d) fins on both surfaces.

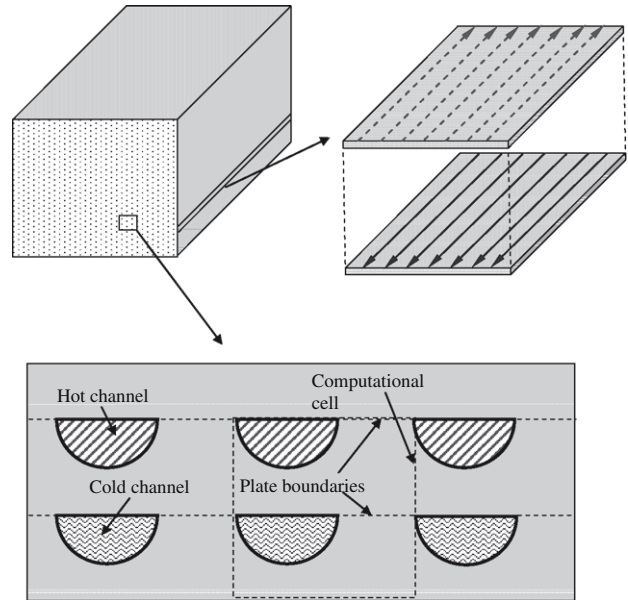


Fig. 2. Printed circuit heat exchanger configuration for the model.

A compact heat exchanger is one that achieves volume reduction compared to conventional (e.g., shell-and-tube) heat exchangers through special design features. The most common design feature to achieve compactness has been small channel size. PCHE achieves small channel size (≈ 1 mm) by chemically etching channels on the surface of metal plate followed by diffusion bonding of the plates to form the heat exchanger core. Flow distributors could be integrated into plates or could be welded outside the core depending on the design. A platelet configuration, where the flow distributors are integrated into the plates, has been selected for the present analysis since it has advantages of a shorter flow distribution region compared to the counter-flow region. Following a small flow distribution region, the flow is purely counter-flow. PCHE are custom-made and optimized for each application; the internal configuration of each PCHE as well as thermal-hydraulic correlations is proprietary information of Heatric. For this analysis, some assumptions on the PCHE internal configuration (including channel diameter, pitch, plate thickness, plate size, and plate configuration) have been made based on engineering judgment. For the analysis, it is assumed that the internal PCHE configuration is represented by a wavy-fin plate heat exchanger with corresponding heat transfer and pressure drop correlations [6]. The modifications have been made to a wavy-fin configuration to account for the PCHE specific features, such as the semi-circular channels and different zigzag channel angles.

4. Materials of construction

The IHX of the NGNP is required to withstand high-temperatures (850–950 °C) for long-life without mechanical property degradation and to resist corrosion/oxidation and erosion from a fast flowing impure helium coolant. The primary materials that can withstand such high-temperatures are nickel-based superalloys. The assessment included four primary candidate alloys namely, Alloy 617 (UNS N06617), Alloy 230 (UNS N06230), Alloy 800H (UNS N08810), and Hastelloy X (UNS N06002) for the IHX. Some of the factors addressed in this study are the tensile, creep, fatigue, creep fatigue, and toughness properties for the candidate alloys, plus thermal aging effects on the mechanical properties, American Society of Mechanical Engineers (ASME) Code compliance information,

and performance of the alloys in helium containing a wide range of impurity concentrations [7].

Among the four candidate materials, Alloy 800H is code certified for temperatures only up to 760 °C for use in nuclear systems and, therefore, the temperature limit is not high enough for application of this alloy in the NNGP IHX. Neither Alloy 617 nor Alloy 230 is currently allowed in ASME Code Section III, although both are allowed in Section VIII, Division 1 (for non-nuclear service). A draft code case for Alloy 617 has been developed but is not yet approved by the ASME Code. A limited database exists for Hastelloy X. Since the high-temperature scaling in Hastelloy X has not been adequate, a modified version Hastelloy XR, has been developed in programs conducted in Japan for which the U.S. has little access for either evaluation or for ASME Code qualification.

Specific conclusions pertaining to materials databases for Alloys 617 and 230 are as follows:

- Alloy 617: Composition refinement is necessary to achieve consistent mechanical properties and for precise evaluation of microstructural effects on mechanical performance. There is a need to generate additional mechanical property data, especially of creep fatigue behavior with and without hold time. The analysis showed that the damage under creep-fatigue conditions is much more than predictions based on the linear rule. Additional data on creep-fatigue under different loading scenarios are needed to develop a predictive capability on creep fatigue damage in the alloy, especially in helium purity levels typical of gas-turbine-based HTGRs. There is a need to establish corrosion regimes in helium with impurity levels anticipated in gas-turbine-based reactor system. Microstructural and mechanical property characterizations are needed for thin section materials, especially for use in compact HXs. It is necessary to validate the effect of system pressure on the corrosion performance of the alloy in impure helium. Tests are needed to verify that the tensile, creep, and creep-fatigue strengths of the diffusion bonded Alloy 617 joints used in the PCHE are adequate.
- Alloy 230: Limited data are currently available on the mechanical properties of the alloy. Data on long-term aging effects on the mechanical property need to be generated. There is lack of information on the long-term corrosion performance of the alloy in helium of relevant impurity levels. Microstructural and mechanical property characterizations are needed for thin section materials, especially for use in compact HXs. The effect of system pressure on the corrosion performance of the alloy in impure helium needs evaluation.

Significant R&D will be needed to qualify Alloy 617 under ASME Code Section III for high-temperature applications, even though some design-relevant material properties are given in the draft code case for temperatures up to 982 °C. The ratcheting rules, that were limited to <650 °C in the draft code case, need to be expanded to allow higher temperatures. At present, there is an insufficient database for Alloy 230 to develop a code case for elevated temperature application. If the IHX is classified as a Class 2 or Class 3 component, new Code Cases need to be developed for high-temperature applications.

5. Thermal-hydraulic calculations

5.1. Printed circuit heat exchanger

The thermal-hydraulic calculations for PCHE are organized in the following way. First, the calculations are performed for “base case” for which the hot and cold fluid parameters are specified

Table 1
Gas-to-gas base case parameters.

Flow conditions	Value	Units
Hot side fluid	He	
Hot side inlet temperature	900	°C
Hot side outlet temperature	575	°C
Hot side inlet pressure	7.0	MPa
Hot side flow rate	26.7	kg/s
Cold side fluid	He	
Cold side inlet temperature	558	°C
Cold side inlet pressure	1.95	MPa
Cold side flow rate	26.7	kg/s
<i>Heat exchanger parameters</i>		
HX type	PCHE	
Unit (plate) length	0.6	m
Unit (plate) width	1.5	m
Unit height	0.6	m
Channel diameter	1.6	mm
Pitch-to-diameter ratio	1.5	
Plate thickness-to-diameter ratio	1.33	
HX core material	Alloy 617	

and the HX configuration is assumed. Then, a sensitivity study is performed to determine the effects of the different parameters. Table 1 defines the base case parameters used in the calculations. Table 2 and Fig. 3 show the results of the “base case” calculations. The required number of HX units is artificially presented as non-integer numbers (for better comparison with the results below). In reality, results in Table 2 suggest that 20 units would be needed to achieve the required heat transfer capacity.

5.1.1. Effect of channel diameter

In order to investigate the effect of the channel diameter on the IHX sizing and performance the channel diameter was varied while all other parameters were kept the same as defined in the base case above. Since input data specifies pitch-to-diameter and plate thickness-to-diameter ratios, actual channel pitch and plate thickness changed proportional to the channel diameter in this study. Fig. 4 shows the results of the channel diameter sensitivity study.

5.1.2. Effect of construction material

Among the candidate alloys, the difference in HX performance is very small. This is due to the fact that for the analyzed conditions

Table 2
Gas-to-gas base case results.

Parameter	Value	Units
HX total heat duty	45.06	MW
Required number of HX units	19.41	
Cold side outlet temperature	883	°C
Hot side pressure drop	25.6	kPa
Cold side pressure drop	43.7	kPa

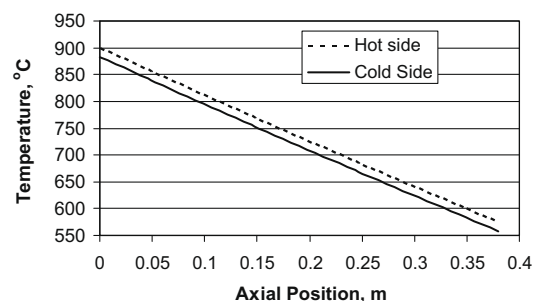


Fig. 3. Temperature profiles for base case.

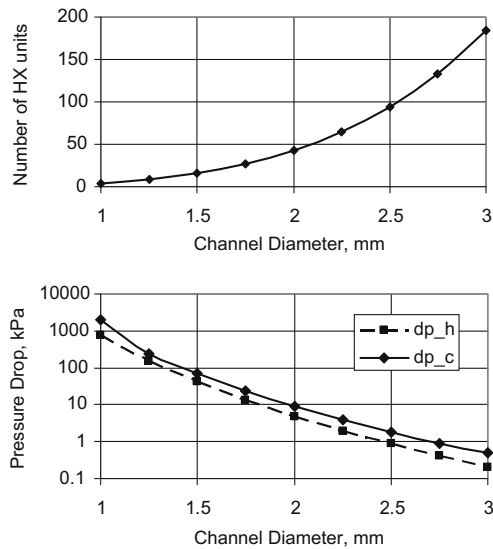


Fig. 4. Effect of PCHE channel diameter on HX size and pressure drop.

the thermal resistance of the plate in PCHE is about an order of magnitude lower than the thermal resistance of the gas inside the channels. Thus, variation of plate thermal conductivity has a minimum effect on the overall thermal resistance. Alloy 617 was selected for the base case, based on expected better mechanical properties at those temperature conditions, and not on the thermal-hydraulic HX performance.

5.1.3. Effect of reactor outlet temperature

In this analysis, the reactor outlet (hot side IHX inlet) temperature has been varied in the range ± 100 °C around the base case value. In order to keep the HX heat duty the same, the hot side outlet temperature has been changed such that ΔT on hot side would be constant. Also, the temperature difference between the hot and cold flow at the cold side inlet has been kept constant. This approach provides that any change in HX performance is solely due to change in gas and metal properties, mainly thermal conductivity, and not due to changed heat load or other factors. Higher thermal conductivity at higher temperatures enhances heat transfer resulting in smaller required HX volume.

5.1.4. Effect of intermediate loop pressure

In this study the intermediate loop (IHX cold side) pressure has been varied from 1 to 8 MPa. Since the intermediate fluid (helium) is closely approximated by ideal gas at these conditions, its properties do not change much with pressure, except for the density. Therefore, the heat transfer HX performance does not change much with the pressure. The pressure drop, on the other hand, is mainly affected by the flow velocity, which is defined by the density. So, the cold side pressure drop changes significantly (from 100 to 10 kPa) with the pressure.

5.1.5. Effect of nitrogen–helium mixture in secondary loop

In this study, the secondary loop fluid has been changed to the nitrogen–helium mixture (80%N₂–20%He). The primary side conditions (fluid, flow rate, temperatures and inlet pressure) as well as HX parameters (number of units and configuration) has been fixed as for the base case above. The cold side inlet temperature was varied parametrically while the inlet pressure was fixed at 7 MPa. The code calculated the required N₂–He mixture flow rate and outlet temperature, as well as pressure drops on both sides (Fig. 5).

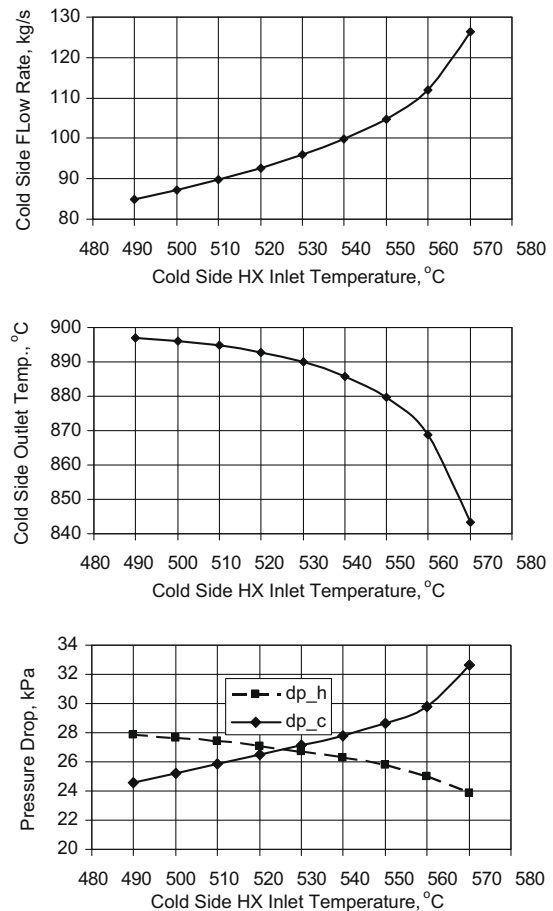


Fig. 5. Results for nitrogen–helium mixture.

5.2. Shell-and-tube IHX

The IHX gas-to-gas calculations were repeated for shell-and-tube HX. Table 3 shows the base case parameters and results of the calculations. Figs. 6 and 7 show the results of the sensitivity analysis of different parameters on IHX performance, similar to those performed for PCHE. Table 4 shows the comparison between PCHE and shell-and-tube heat exchangers. The results for the shell-and-tube heat exchanger are reported for bare and finned tubes. Table 4 demonstrates the compactness of PCHE compared to shell-and-tube HX.

6. Stress calculations

6.1. Printed circuit heat exchanger

Thermal and stress analyses of a three-dimensional honeycomb structure like the compact IHX are highly complex. To simplify, a 0.38 m long (excluding the 0.11 m long header regions at the inlet and outlet ends) unit cell of the compact IHX core was considered for thermal and stress analyses. Half of the cross-section of a repeating unit cell from the reference geometry was used in the analysis. The base case with the reactor outlet temperature of 900 °C, the reactor outlet pressure of 7 MPa, and the intermediate loop pressure of 2 MPa was considered for stress analysis. First, a steady-state thermal conduction analysis was carried out using the heat fluxes for both the hot and cold channels as a function of axial location reported in an earlier Section. Next, stress analyses were conducted with and without thermal stress contribution.

Table 3
Shell-and-tube IHX base case parameters and results.

Flow conditions	Value	Units
Hot side fluid	He	
Hot side inlet temperature	900	°C
Hot side outlet temperature	575	°C
Hot side inlet pressure	7.0	MPa
Hot side flow rate	26.7	kg/s
Cold side fluid	He	
Cold side inlet temperature	558	°C
Cold side inlet pressure	1.95	MPa
Cold side flow rate	26.7	kg/s
<i>Heat exchanger parameters</i>		
HX type	Shell-and-tube	
Tube length	6.0	m
Tube inner diameter	10	mm
Tube outer diameter	14	mm
Pitch-to-diameter ratio	1.33	
Number of fins on inner tube surface	0	
Number of fins on outer tube surface	0	
Tube side	Hot He	
Tube material	Alloy 617	
<i>Results</i>		
HX total heat duty	45.062	MW
Required number of tubes	174,800	
Required shell diameter (1 unit)	8.175	m
Cold side outlet temperature	883	°C
Hot side pressure drop	0.052	kPa
Cold side pressure drop	0.055	kPa

coldest point is small (≈ 5 °C). However, there is a large axial temperature gradient from the hot to the cold end, as expected.

6.3. Stress analysis

Two stress analyses, both assuming linear elastic behavior, were conducted using the finite element code ABAQUS. First, a primary (pressure) stress analysis was conducted without any contribution from thermal stresses. Second, a secondary (thermal) stress analysis was conducted without the pressure stresses. In the second analysis, the temperature data calculated in the thermal conduction analysis were input into the ABAQUS code. In both cases, the axial displacement (u_z) was set equal to zero at one end ($z = 0$) and generalized plane strain deformation (i.e., $u_z = \text{constant}$) was assumed at the other end. Similar boundary conditions were used at the other symmetry planes.

6.3.1. Primary stresses

The primary stress distribution at either end of the IHX is identical and is shown in Fig. 10. The stresses are higher near the hot channel than in the cold channel because the pressure in the hot channel is 7 MPa and the pressure in the cold channel is 1.9 MPa. The maximum von Mises effective stress is 22 MPa which occurs locally at the edge of the hot coolant channel. A slightly higher maximum stress (22.5 MPa) occurs at a section in the middle. However, most of the structure is under relatively low stress. There is little variability in the stress distribution along the length of the IHX. Note that the peak stress is not relevant for satisfying ASME primary stress requirements, as will be discussed later.

6.3.2. Secondary (thermal) stresses

The distribution of effective von Mises stress at the hot and cold ends of the IHX due to thermal loading alone are plotted in Figs. 11 and 12, respectively. A peak stress of 52 MPa occurs at the periphery of the hot channel where the temperature is 880 °C. The peak stress at the cold end is 116 MPa (Fig. 12), which also occurs at the periphery of the hot channel (Fig. 11) where the temperature is 565 °C (Fig. 8).

6.3.3. ASME Code compliance calculations

Since the IHX operates in a high-temperature environment where creep deformation is important, Subsection NH of ASME Code, Section III is applicable. However, there are several problems with applying ASME Section III code rules to the compact IHX structure. First, the use of the primary candidate structural Alloy 617 is currently not approved in Subsection NH. There is a draft Code Case (still unapproved) for designs using Alloy 617. The draft Code Case was patterned after relevant portions of Subsection NH, and limited to Alloy 617, temperature of 982 °C (1800 °F), and maximum service life [total life at temperatures above 427 °C (800 °F)] of 100,000 h or less. However, the ratcheting rules in the draft Code Case is limited to a maximum temperature of 649 °C. The draft Code Case focused on Alloy 617 because it was a leading candidate high-temperature structural material, and there was a significant material properties database at the temperature of interest. We have used the allowable stress values from this draft Code Case for the present report. Second, there is an additional problem because the code rules were formulated for shell-type structures in which one of the dimensions (thickness) is much smaller than the other two. In contrast, the compact IHX is a three-dimensional honeycomb structure in which there is no unique way of determining membrane and bending stresses, the limits on which form the bases of many of the Code rules.

In the absence of any guidance on designing these kinds of structures, we have made some ad hoc assumptions to define the membrane and bending stresses by taking advantage of the thinness of the walls separating the channels. The ASME Code

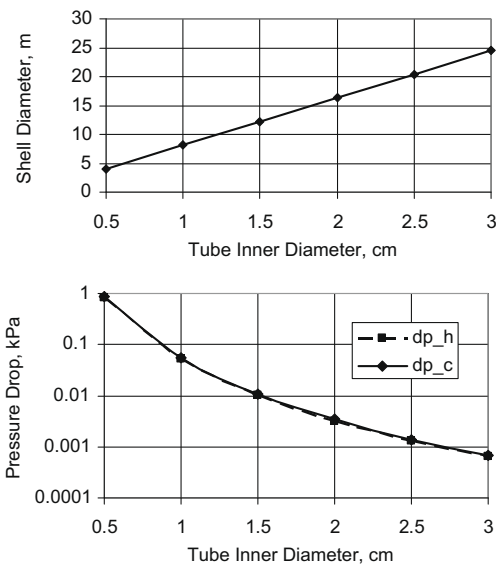


Fig. 6. Effect of tube diameter on shell-and-tube IHX performance.

6.2. Thermal conduction analysis

The structural material considered was Alloy 617 whose thermal conductivity was input as a function of temperature in the finite element code (ABAQUS). In the finite element analysis (FEA), the total length of the compact IHX was divided into 11 sections and average values of the HTC (heat transfer coefficient) and gas temperature were used in each section. In the FEA, the total length of the compact IHX was divided into 11 sections and average values of the HTC and gas temperature were used in each section.

The FEA-calculated distributions of temperatures at the hot and cold ends of the IHX are plotted in Figs. 8 and 9, respectively. Note that the temperature gradient at each end from the hottest to the

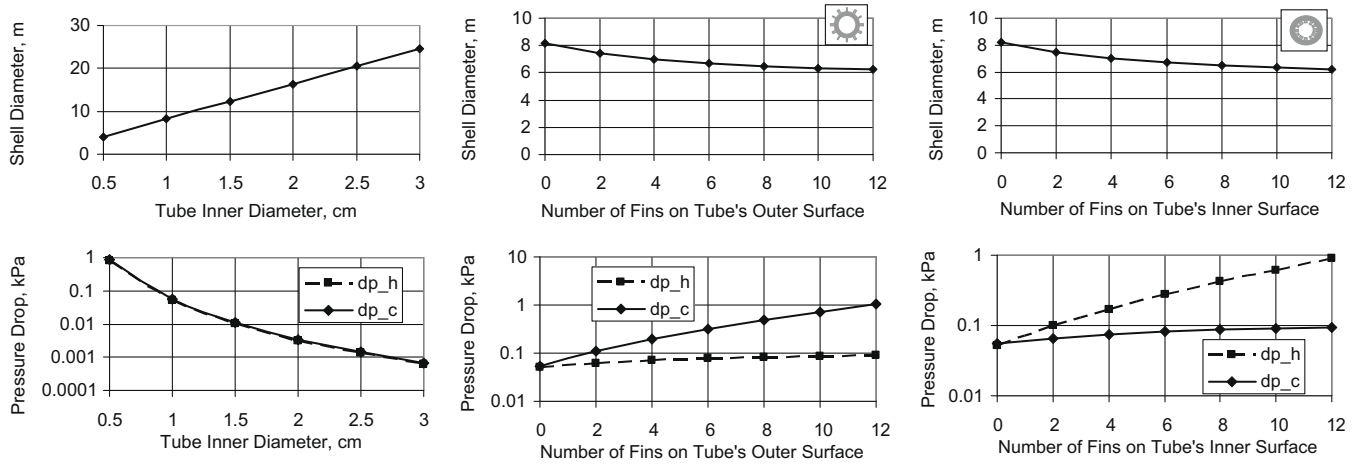




Fig. 7. Effect of (a) tube diameter, (b) outer tube fins, and (c) inner tube fins on IHX performance.

Table 4
Comparison of PCHE and shell-and-tube IHX designs.

Heat exchanger type	PCHE	Shell-and-tube	
			
Unit dimensions	0.6 m (L) × 1.5 m (W) × 0.6 m (H)	6 m (L) × 8.17 m (D)	6 m (L) × 3.31 m (D)
Number of units	20	1	1
Total HX volume, m ³	10.5	314.5	51.6
Pressure drop, hot/cold sides, kPa	25.6 43.7	0.05 0.05	3.2 3.7

(Subsection NH) requires that for normal operation and upset conditions

$$P_m \leq S_{mt}, \tag{1}$$

$$P_L + P_b \leq K S_m, \text{ and} \tag{2}$$

$$P_L + P_b / K_t \leq S_t, \tag{3}$$

where P_m is primary membrane stress, $P_L + P_b$ is the membrane plus bending primary stress, S_{mt} is the time and temperature dependent allowable stress, S_m is time independent allowable stress, S_t is time dependent allowable stress, and K_t accounts for relaxation of extreme fiber bending stress due to creep. The factor is given by

$$K_t = (K + 1) / 2, \tag{4}$$

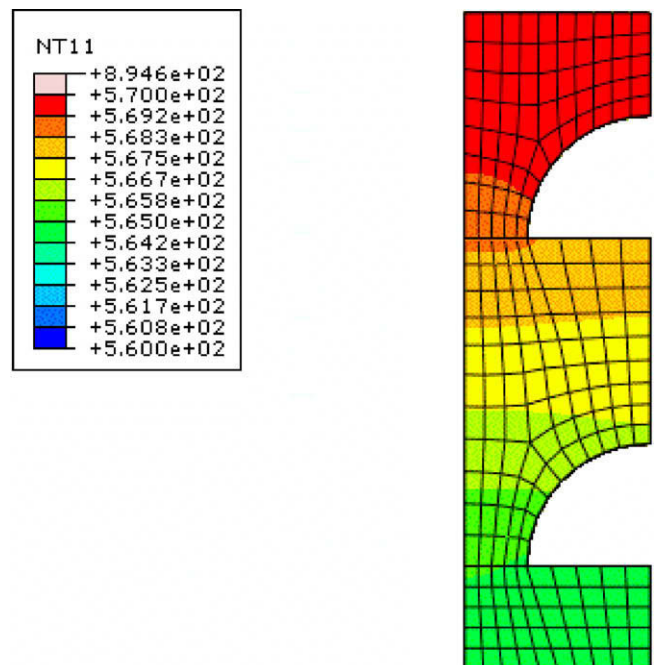
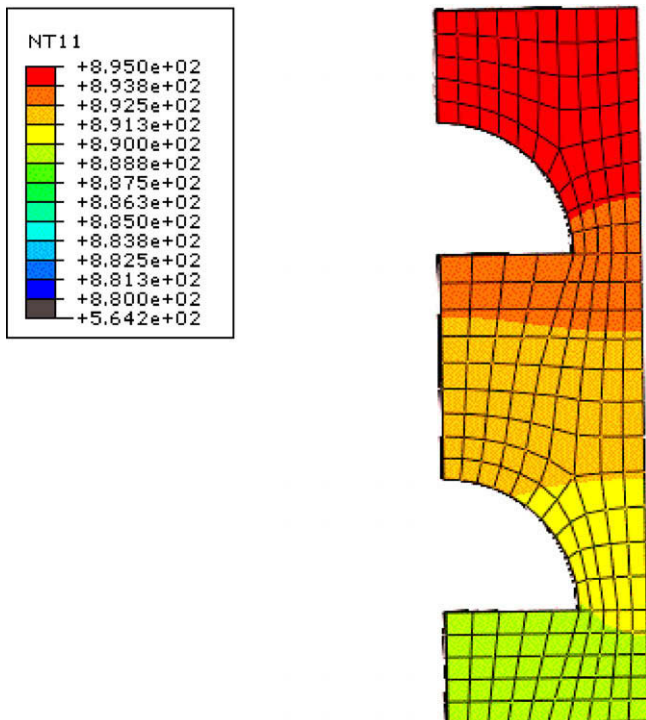


Fig. 8. Temperature distribution (in °C) in the compact IHX at the hot end.

Fig. 9. Temperature distribution (in °C) in the compact IHX at the cold end.

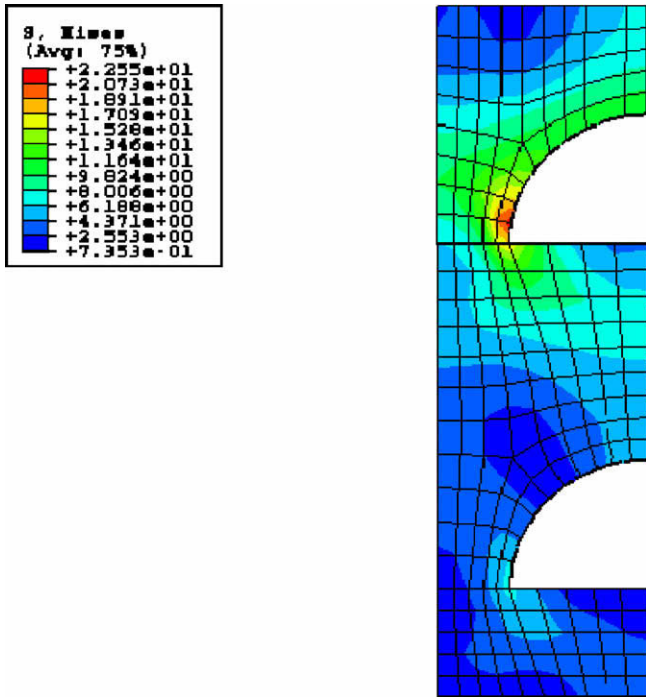


Fig. 10. Distribution of primary (pressure) von Mises effective stress (in MPa) at either end of the compact IHX.

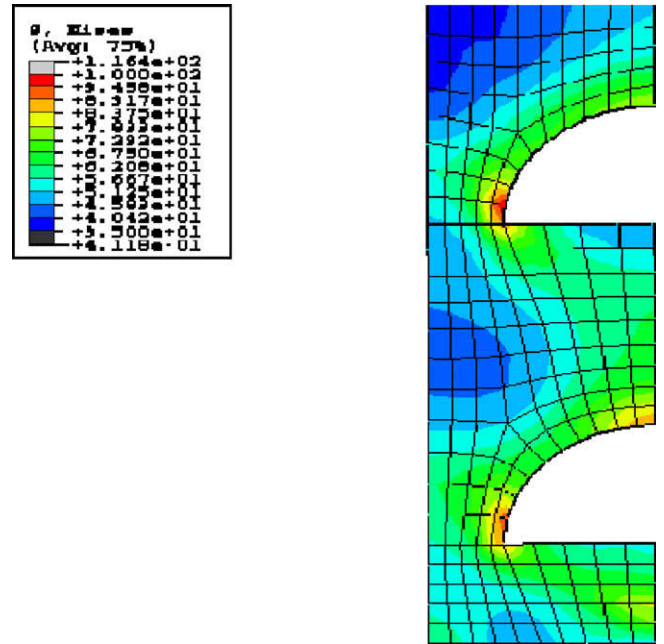


Fig. 12. Distribution of von Mises effective stress (in MPa) due to thermal loading at the cold end of the IHX.

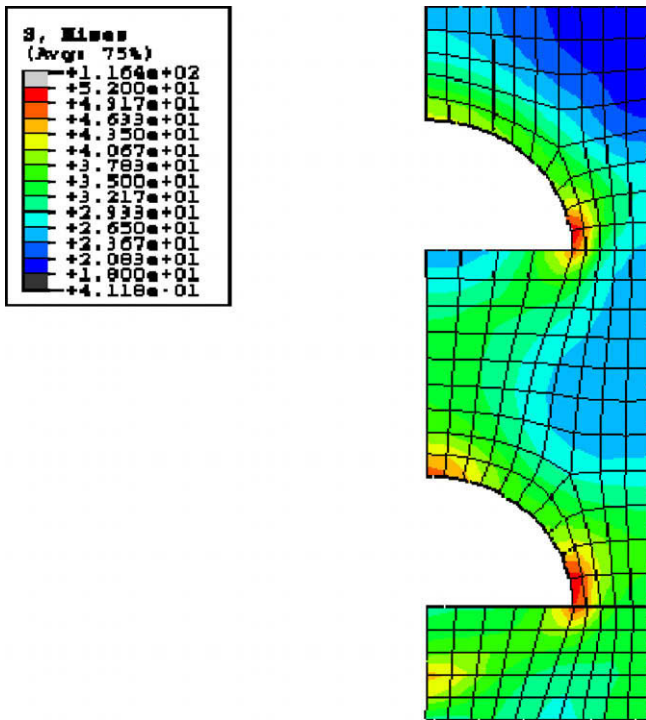


Fig. 11. Distribution of von Mises effective stress (in MPa) due to thermal loading at the hot end of the IHX.

where K is the bending shape factor. For solid rectangular sections, $K = 1.5$. However, for a hollow section like the compact IHX, it should be <1.5 . To be conservative, we have assumed $K = 1$. The calculated values of P_m and $P_L + P_b$ for the two paths considered in Fig. 13(a) and (b) are plotted on the allowable stress intensities vs. time and temperature plot for Alloy 617 in Fig. 13(a) and (b),

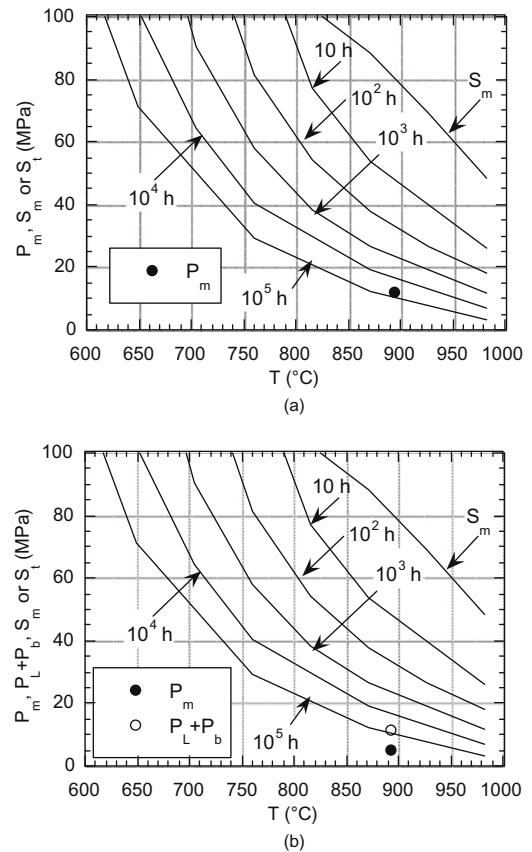


Fig. 13. Calculated P_m and $P_L + P_b$ values along paths across the (a) hot channel-to-hot channel ligament and (b) hot channel-to-cold channel ligament for the IHX plotted on the allowable stress intensities vs. temperature and time curves for Alloy 617.

respectively. It is evident that the $P_L + P_b$ limit is the controlling criterion for life of the hot-to-cold channel ligament. The maximum

allowable design lives of the hot channel-to-hot channel and the hot channel-to-cold channel ligaments are 80000 and 90000 h, respectively, for the assumed reactor outlet conditions. These design lives are based on design curves given in the draft Code Case for Alloy 617 and may have to be reduced if thickness effects are taken into account.

6.3.4. Diffusion-bonded joint

If the IHX is fabricated by diffusion bonding, the bond strength may become the controlling factor for life. The distributions of the von Mises effective stress along the diffusion joint and the stress normal to the joint are plotted in Fig. 14(a). Although the integrated net force due to the normal stress across the joint is zero, the von Mises effective stress is relatively constant. Also, half of the joint is under normal tensile stress, which is balanced by compressive stress on the other half. The average value of the von Mises stress is plotted on the allowable stress intensities vs. time and temperature plot for Alloy 617 in Fig. 14(b). Currently, we have no data on the high-temperature creep rupture properties of diffusion-bonded Alloy 617 plates. If the bond strength is as good or better than the base material, the design life of the joint is greater than 100000 h.

6.4. Shell-and-tube IHX

In contrast to the compact IHX, the shell-and-tube design is relatively easy to analyze. The effect of the tube end conditions, which will add some complications to the analyses, is ignored for the present. We have analyzed the base case for the reference design of the shell-and-tube IHX, which consists of 6 m long, 10 mm ID, 14 mm OD Alloy 617 tubes arranged in a triangular lattice inside

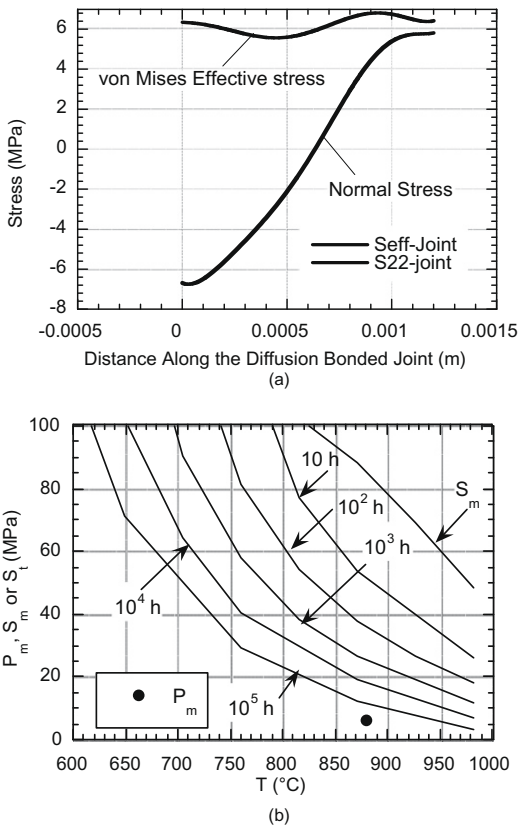


Fig. 14. (a) Variation of von Mises effective stress along a path on the diffusion joint and (b) the primary membrane stress intensity P_m and the allowable stress intensities vs. temperature and time curves for Alloy 617.

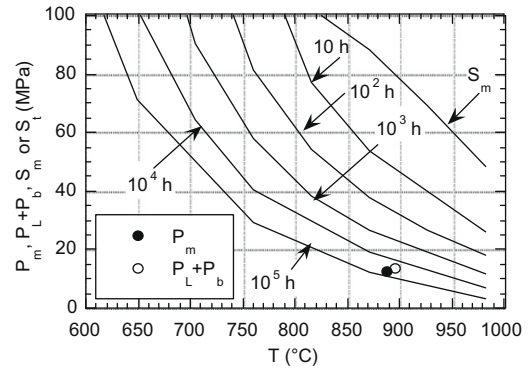


Fig. 15. Calculated P_m and $P_L + P_b$ values for the shell-and-tube IHX plotted on the allowable stress intensities vs. temperature and time curves for Alloy 617.

a shell. The reactor outlet temperature and pressure are 900 °C, and 7 MPa, respectively, and the secondary side pressure is 1.95 MPa and the inlet cold temperature is 575 °C.

6.4.1. Primary stresses

The membrane primary stress (P_m) due to the base case primary and secondary side pressures is 12.6 MPa and the maximum average wall temperature 888 °C. The membrane plus bending primary stress ($P_L + P_b$) at the ID surface is 13.6 MPa and the peak temperature at this location is 896 °C. The calculated values of P_m and $P_L + P_b$ are plotted on the allowable stress intensities vs. time and temperature plot for Alloy 617 in Fig. 15. It is evident that the $P_L + P_b$ limit is the controlling criterion for life and the maximum allowable design life for the shell-and-tube IHX is 20000 h for the assumed reactor outlet conditions. This design life is somewhat less than that of the compact IHX for the same reactor outlet conditions.

7. Summary

Thermal-hydraulic calculations showed that both PCHE and shell-and-tube design are feasible concepts for the considered application. The results also show that for shell-and-tube configuration, significant heat exchanger volume reduction could be achieved by enhancing the surface area by means of surface fins. PCHE technology shows even greater heat exchanger volume reduction compared to the shell-and-tube configuration even with the surface fins. The effect of various heat exchanger design parameters and materials was calculated.

For a reactor outlet temperature and pressure of 900 °C and 7 MPa, respectively, and a secondary side inlet temperature and pressure of 575 °C and 1.95 MPa, respectively, the allowable design life (based on in-air tensile and creep rupture strengths of Alloy 617) of the compact IHX is 80000 h and that of the shell-and-tube IHX (for the tube size selected) is 20000 h. These design lifetimes are based on analyses of the IHX core and further reduction in life may result from interaction of the core region with the header region. The design lifetimes may also decrease, if thin section creep properties (which are generally less than those of thicker material) are considered. In addition, the effect of impure helium on creep properties needs to be incorporated in the design data and in lifetime calculations.

It is noted though that the analyzed PCHE configuration may not be representative of the exact configuration developed for this application, if such comprehensive development would be carried out. For example, some assumptions on the internal PCHE configuration have been made without the mechanical design considerations.

References

- [1] C.B. Davis, C.H. Oh, R.B. Barner, S.R. Sherman, D.F. Wilson, Thermal-Hydraulic Analyses of Heat Transfer Fluid Requirements and Characteristics for Coupling A Hydrogen Production Plant to a High-Temperature Nuclear Reactor, INL/EXT-05-00453, 2005.
- [2] E.A. Harvego, Evaluation of Next Generation Nuclear Power Plant (NGNP) Intermediate Heat Exchanger (IHX) Operating Conditions, Idaho National Laboratory Report INL/EXT-06-11109, 2006.
- [3] P.E. MacDonald, P.D. Bayless, H.D. Gougar, R.L. Moore, A.M. Ougouag, R.L. Sant, J.W. Sterbentz, W.K. Terry, 2004, The next generation nuclear plant – insights gained from the ineel plant design studies, in: Proc. ICAPP-04, Pittsburgh, PA, 2004, p. 349.
- [4] Heatric web site, <www.heatric.com>.
- [5] A. Moisseytsev, Passive Load Follow Analysis of the STAR-LM and STAR-H2 Systems, Ph.D. Dissertation, College Station, TX, 2003.
- [6] W.M Kays, A.L London, Compact Heat Exchangers, McGraw-Hill, New York, 1984.
- [7] K. Natesan, A. Moisseytsev, S. Majumdar, P.S. Shankar, Preliminary Issues Associated with the Next Generation Nuclear Plant Intermediate Heat Exchanger Design, Argonne National Laboratory Report, ANL/EXT-06/46, 2006.